Alginate/Chitosan Particle-Based Drug Delivery Systems for Pulmonary Applications

pharmaceutics

MDPI

Article

Alginate/chitosan bionanocomposite nanoparticles for pulmonary applications

Marcus Hill [1], Matthew Twigg [2], Emer A. Sheridan [3], John G. Hardy [4, 5,*], J. Stuart Elborn[6,*], Clifford C. Taggart [2,*], Christopher J. Scott [7,*], and Marie E. Migaud [1,8,*]

[1] School of Pharmacy, Queen's University Belfast Queen's University Belfast, Belfast, BT7 1NN, UK; mhill11@qub.ac.uk (M.H.); mmigaud@health.southalabama.edu (M.E.M.)
[2] Airway Innate Immunity Group (AiiR), Wellcome Wolfson Institute of Experimental Medicine, School of Medicine, Dentistry and Biomedical Sciences, Queen's University Belfast, 97 Lisburn Road, Belfast, BT9 7BL, Northern Ireland, UK.; m.twigg@qub.ac.uk (M.T.), c.taggart@qub.ac.uk (C.C.T.), c.scott@qub.ac.uk (C.J.S.)
[3] Lancashire Teaching Hospitals NHS Trust, Emergency Department, Royal Preston Hospital, Sharoe Green Lane, PR2 9HT, UK; emer.a.barr@gmail.com (E.A.S.)
[4] Department of Chemistry, Lancaster University, Lancaster, Lancashire, LA1 4YB, UK; j.g.hardy@lancaster.ac.uk (J.G.H.)
[5] Materials Science Institute, Lancaster University, Lancaster, Lancashire, LA1 4YB, UK; j.g.hardy@lancaster.ac.uk (J.G.H.)
[6] School of Medicine, Dentistry and Biomedical Sciences, Queen's University Belfast, 97 Lisburn Road, Belfast, BT9 7BL, Northern Ireland, UK; s.elborn@qub.ac.uk (J.S.E.)
[7] Centre for Cancer Research and Cell Biology, School of Medicine, Dentistry and Biomedical Sciences, Queen's University Belfast, 97 Lisburn Road, Belfast, BT9 7BL, Northern Ireland, UK; c.scott@qub.ac.uk (C.J.S.)
[8] USA Mitchell Cancer Institute, University of South Alabama, Mobile, AL 36604, USA; mmigaud@health.southalabama.edu (M.E.M.)
* Correspondence: j.g.hardy@lancaster.ac.uk (J.G.H.); s.elborn@qub.ac.uk (J.S.E.); c.taggart@qub.ac.uk (C.C.T.); c.scott@qub.ac.uk (C.J.S.); mmigaud@health.southalabama.edu (M.E.M.); Tel.: +1-251-410-4938.

Received: date; Accepted: date; Published: date

Abstract: Cystic fibrosis (CF) is a complex, potentially life threatening disease. Here we describe the results of our investigation on the development of alginate/chitosan nanoparticles for pulmonary applications. In the first paradigm, tobramycin loading and release was investigated to treat a clinically relevant model bacteria (*Pseudomonas aeruginosa*) in vitro, and in the second paradigm the nanoparticles were functionalized with secretory leukocyte protease inhibitor (SLPI) which were shown to help inhibit the inflammatory response associated with lung infections and enhance their interactions with mucus in vitro.

Keywords: biomedical applications; drug delivery systems; nanoparticles; antimicrobial.

1. Introduction

Cystic fibrosis (CF) is a complex, potentially life threatening disease which is manifested through mutations in the cystic fibrosis transmembrane conductance regulator (CFTR) [1]. The protein product of this gene functions as a cyclic AMP (cAMP) dependent transmembrane chloride (Cl^-) channel. It is responsible for the transport of ions across the apical membrane of exocrine epithelial cells [2]. The protein shows widespread expression across the epithelial lining of most exocrine glands, though is mainly expressed in cells of the small intestine, airways, vas deferens and ducts of the pancreas [3-6]. The mutations present in the CFTR gene have been shown to lead to the subsequent loss of Cl^- transport in these cell types. The pulmonary environment has been shown to be one of the most largely effected by the loss of Cl^- channel activity [7] concomitant with a decrease in volume of the airway surface liquid (ASL) causing the accumulation of thickened mucus in the

pulmonary environment (**Figure 1**) [8,9]. This is believed to increase the susceptibility of the lung to infection by organisms including *Pseudomonas aeruginosa*, *Haemophilus influenza* and *Staphylococcus aureus* [10]. Early infecting strains such as *S. aureus* are usually cleared by antibiotic therapy though are believed to facilitate chronic colonization by *P. aeruginosa* [11]. Chronic colonization with *P. aeruginosa* coincides with increasing antibiotic resistance and the emergence of *P. aeruginosa* as the dominant infecting organism over time [12].

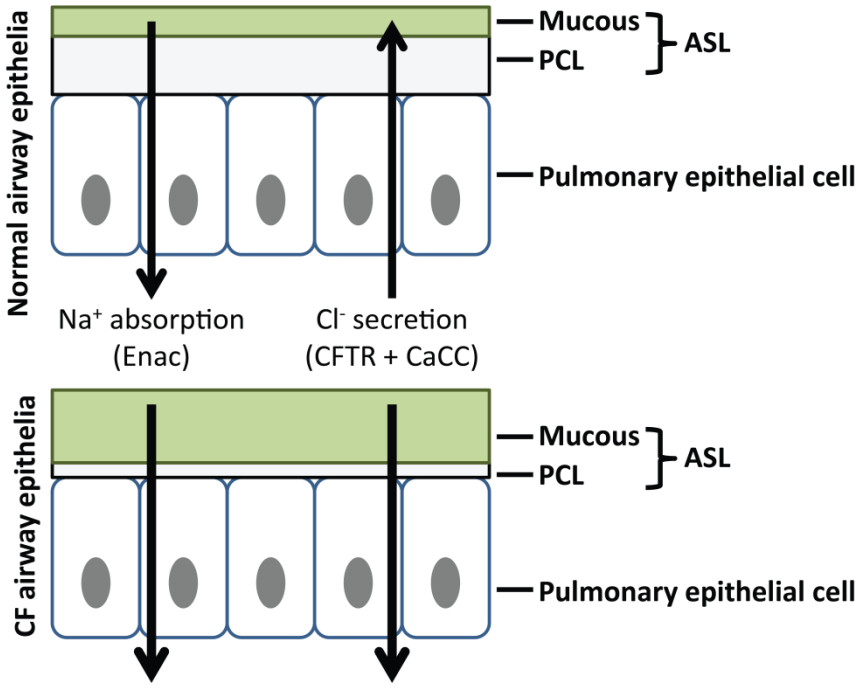

Figure 1. Events linking altered lung airway surface layer (ASL) volumes to decreased mucociliary clearance. A) Normal airway surfaces contain a small mucus layer which facilitates entrapment of inhaled particles and pathogens. ASL autoregulation leads to the maintenance of the pericilliary liquid layer (PCL) which allows movement and clearance of inhaled particles and pathogens. B) Hyperabsorption of Na^+ and ineffective Cl^- secretion in the CF airway cause depletion of ASL, collapse of the cilia in the PCL and adherence of concentrated mucus in the airways. Adapted from [9].

Chronic infection with *P. aeruginosa* is one of the most significant events in the pathogenesis of cystic fibrosis [13]. Tobramycin, is the treatment of choice for those patients with chronic *P. aeruginosa* infection who are deteriorating despite regular colistimethate sodium [14,15]. It is one of the most effective treatments for pulmonary exacerbations and is generally delivered through nebulization at a dose of 300 mg twice daily. The pharmacokinetic parameters are similar to other aminoglycoside drugs resulting in rapid renal excretion [16]. As with other aminoglycosides tobramycin shows no activity against gram positive organisms such as *S. aureus* therefore early CF antibacterial therapies often focus on administration of anti-staphylococcal prophylactic antibiotics [17].

Clinical treatment with tobramycin involves twice daily administration of high doses of drug due to the high absorption and short plasma half-life of the drug [18]. One of the main problems with CF therapy is non-compliance. Non-compliance with antibiotic regimens can lead to antibiotic failure [19], therefore altering the dosing schedule of Tobramycin from twice daily to once daily may in part address compliance issues. Another concern with prolonged tobramycin treatment is the potential toxicity experienced due to the ototoxic and nephrotoxic property of the drug [20,21]. Nephrotoxicity is often associated with parenteral aminoglycoside therapy but there is limited evidence of nephrotoxicity and ototoxicity in clinical trials with nebulized tobramycin [22]. With longer durations of therapy there is an increased potential risk of nephrotoxicity. Therefore the

development of delivery systems for tobramycin which could reduce the dosing frequency of the drug while also reducing systemic toxicity upon prolonged exposure may be of clinical benefit.

The CF lung provides a further barrier to efficient drug delivery due to the presence of a thick mucus layer on the epithelial lining [23]. This is due to the altered salt transport system within the CF lung which results in increased dehydration and mucus viscosity with delayed mucus clearance [24]. Furthermore, *P. aeruginosa* forms a thick alginate based biofilm which provides increased resistance to antibacterial therapy [11].

A further complication arises from the enhanced pro-inflammatory response to infection which causes increased infiltration of neutrophils to the site of bacterial colonization [25]. Neutrophils promote the pro-inflammatory response to infection through the release of various pro-inflammatory proteases such as neutrophil elastase (NE) which can overload the endogenous anti-protease host defenses leading to tissue damage and loss of respiratory function [12]. There is therefore interest in the development of drug delivery systems which can enhance the antibacterial activity of the delivered payload through increased accumulation at the site of infection while reducing the aberrant inflammatory response to infection.

The secretory leukocyte protease inhibitor (SLPI) is an 11.7 kDa protein which is naturally expressed as part of the innate immune response in humans [26]. SLPI is naturally expressed in a number of bodily secretions including nasal, pulmonary, salivary and seminal secretions [27-30]. SLPI has been shown to display potent anti-inflammatory activity through inhibition of a number of endogenous serine proteases including NE [31]. Due to the high association rate constant for NE it is believed SLPI acts as the primary inhibitor of NE in vivo [12]. Studies have shown therapeutic administration of recombinant SLPI (r-SLPI) to CF patients can reduce the inflammatory response by lowering active levels of NE while also reducing NE mediated IL-8 production which is involved in the recruitment of pro-inflammatory mediators to the site of disease [32,33]. SLPI has also been shown to reduce inflammation through inhibition of NF-κB signaling [34].

Here we describe the results of our investigation on the development of alginate/chitosan nanoparticles for pulmonary applications. In the first paradigm, tobramycin loading and release was investigated, and in the second paradigm the nanoparticles were functionalized with secretory leukocyte protease inhibitor (SLPI) to help inhibit the inflammatory response associated with infection (and potentially passively target the nanoparticles through binding with anionic mucins within mucus to provide enhanced targeting to the site of disease due to its cationic nature).

2. Materials and Methods

2.1. Materials

Unless otherwise noted, all chemicals were obtained from Sigma Aldrich, UK. Boric acid, calcium chloride hexahydrate and the Pierce BCA protein assay kit were purchased from Fisher Scientific UK. Tryptone, sodium chloride (bacteriological grade) and yeast extract were purchased from Oxoid Ltd., Basingstoke, Hampshire, England. Ethanol was purchased from J.T Baker, Netherlands. Recombinant human neutrophil elastase was purchased from the Elastin Products Company (EPC) Owensville, MO, USA. NE substrate (methoxysuccinyl-L-alanyl-alanyl-prolyl-L-valyl-4-nitroanilide) was purchased from Calbiochem, USA. Recombinant human secretory leukocyte protease inhibitor (SLPI) was purchased from Amgen UK. Biotinylated anti-human SLPI antibody was purchased from R&D Systems (Abingdon, Oxon, UK). Sputum from CF patients was obtained anonymously from the adult CF centre at Belfast City Hospital. Sputum samples were in excess to requirements for diagnostic purposes. Permission to use sputum samples (which would have been disposed of) for validation purposes was given by the Director of R&D in Belfast Health and Social Care Trust.

2.2. Preparation of tobramycin loaded alginate/chitosan nanoparticles

Several formulations of tobramycin were tested for their ability to formulate tobramycin loaded nanoparticles with no aggregation. $CaCl_2$ and chitosan were utilized as cationic crosslinkers.

Tobramycin was included in all formulations. Briefly, aqueous solutions of tobramycin (1.5 mg in 3 ml) were added to various amounts of sodium alginate (pH 5.4) while stirring (500 rpm) at room temperature. 1 ml of chitosan (1% v/v glacial acetic acid, pH 5.1) at various concentrations was added while stirring (500 rpm). The nanoparticles were collected by centrifugation at 20,000 g and washed in PBS three times by centrifugation resuspension cycles.

2.3. Nanoparticle characterization

The size and zeta potential analysis of the nanoparticles was determined by dynamic light scattering (DLS) using a Malvern Zetasizer (Nano ZS; Malvern instruments, Malvern U.K). For particle analysis each sample was read in triplicate (10 runs each). The average of three separate samples was taken and the data presented as the mean ± standard deviation. Transmission electron microscopy (TEM) was performed using a JEOL JEM1400 transmission electron microscope at an accelerating voltage of 80 kV. Nanoparticles (0.6 mg/ml) were loaded on a copper grid (Formvar/Carbon 200 μm mesh, Agar Scientific), the moisture wicked off and allowed to dry. 2 μl of uranyl acetate (2% w/v) was added to provide contrast between the nanoparticles and copper grid.

2.4. Conjugation of SLPI to chitosan

Chitosan 0.5 ml (2 mg/ml, in 1% v/v glacial acetic acid) was diluted 1:1 in PBS buffer (25 mM, pH 7.4) and 10 μl of SLPI was added (25 mg/ml). The pH of the solution was adjusted to 5 and the conjugation was initiated by the addition of 1-ethyl-3-(dimethylaminopropyl carbodiimide) (EDC) (2.5 mg/ml) and left stirring for 6 h at room temperature. The SLPI/chitosan conjugate was used instantly for nanoparticle formation with alginate and excess EDC was removed by washing of the nanoparticles through centrifugation resuspension cycles.

2.5. Quantification of SLPI conjugation

Nanoparticles were formulated as described previously and centrifuged at 20,000 g. The supernatant was collected. Blank nanoparticles (not conjugated to SLPI) were also included as a control. The levels of SLPI conjugation achieved were measured with the BCA assay kit (Pierce, UK). 25 μl of control and conjugate nanoparticles were added to 175 μl of BCA reagent A (sodium carbonate, sodium bicarbonate, bicinchoninic acid and sodium tartrate in 0.1 M sodium hydroxide) and B (4% W/W cupric sulphate in water) in a 96 well plate. The plate was then incubated for 60 min at 37ºC. The absorbance of the resultant solution was read at 570 nm and compared to a calibration curve of SLPI.

2.6. Analytical methodology for detection of tobramycin sulphate

Reagent A consisting of 80 mg of ortho-phthaldialdehyde in 1ml of 95% ethanol and reagent B containing 200 μl of boric acid (pH 9.7, 0.4 M), 400 μl β-mercaptoethanol and 200 μl of diethyl ether were mixed. Serial dilutions of tobramycin were prepared in boric acid (pH 9.7, 0.4 M). 100 μl of each tobramycin standard was added to 100 μl of the reagent mixture. The plate was read by fluorescence at $\lambda_{ex}/\lambda_{em}$ 360/460 nm, respectively.

2.7. Quantification of tobramycin release

Drug release was quantified by incubating the nanoparticles in dialysis membranes with a 10,000 Da MWCO at 37˚C with agitation. The release of the tobramycin was quantified by incubating 3 mg of nanoparticles in 1 ml of PBS in the donor compartment with 5 ml of PBS in the receiver compartment. At each time point the PBS was collected and replaced with fresh PBS release medium. Quantification of the tobramycin release was performed by diluting the release medium 1:1 with Boric acid (0.4 M pH 9.7) prior to derivatization with ortho-phthaldialdehyde (80 mg) in a solution containing 1 ml of 95% ethanol, 200 μl Boric acid (0.4 M pH 9.7), 400 μl of β-mercaptoethanol and 200 μl diethyl ether. The fluorescent derivative was monitored by fluorescence at $\lambda_{ex}/\lambda_{em}$ 360/460 nm, respectively.

175 *2.8. Minimum inhibitory concentration effect of tobramycin on P. aeruginosa*

176 Broth micro-dilution tests were performed according to NCCLS guide lines. Serial two-fold
177 dilutions of tobramycin (from stock solution which had been sterile filtered with 0.22 μm filter) in
178 100 μl of Luria Bertani (LB) broth were performed on a 96 well plate in the range 0-25 μg/ml for the
179 drug loaded nanoparticles, free tobramycin and the blank nanoparticles as negative control. The
180 actively growing cultures were diluted to an optical density reading of 0.3 (A550) to give a starting
181 inoculum of $2x10^5$ CFU/ml. 100 μl of the starting inoculum ($2x10^5$ CFU/ml) was added to each well of
182 the plate and incubated aerobically at 37°C for 24 h. Positive and negative controls were included in
183 each assay.

184 *2.9. Inhibition of neutrophil elastase by SLPI functionalised alginate/chitosan nanoparticles*

185 Anti-neutrophil elastase activity was monitored by incubation with the human neutrophil
186 elastase (HNE) specific substrate methoxysuccinyl-Ala-Ala-Pro-Val-P-nitroanilide (Sigma, Aldrich,
187 UK). Inhibitions of HNE (Elastin products, Owensville, MO) were measured in the presence and
188 absence of both blank and SLPI conjugated nanoparticles. The assay was carried out by incubating
189 10 μl (10 mg/ml particles) of blank and SLPI conjugated nanoparticles containing 100 μg/ml SLPI
190 with 4 μl of HNE (100 μg/ml). HNE activity was measured by the cleavage of chromogenic
191 methoxysuccinyl-Ala-Ala-Pro-Val-P-nitroanilide substrate by adding 50 μl of 0.2 mM substrate in
192 0.1 M HEPES buffer containing 0.5 M NaCl. Assays were conducted at 37°C and the formation of the
193 fluorescent product (p-nitroaniline) was measured continuously at 405 nm on a BMG-Labtech
194 Fluorstar Optima fluorescent plate reader.

195 *2.10. Preparation of Rhodamine 6G loaded alginate/chitosan nanoparticles*

196 3 ml of a tobramycin stock solution in water (0.5 mg/ml) was added to 3 ml of sodium alginate
197 (3 mg/ml pH 5.4). 250 μl of Rhodamine 6G (2 mg/ml) was then added to the tobramycin alginate
198 mixture. 1 ml of chitosan (1% v/v glacial acetic acid pH 5.1) was added while stirring (500 rpm). The
199 nanoparticles were collected by centrifugation at 20,000 g and washed in PBS three times by
200 centrifugation resuspension cycles.

201 *2.11. Penetration of SLPI functionalised nanoparticles in CF mucus*

202 The penetration of rhodamine loaded nanoparticles with and without SLPI functionalisation
203 was studied in CF mucus. A 500 μl layer of 10% gelatin (Porcine type A Sigma- Aldrich) was added
204 to a 24 well microplate and allowed to harden. 500 μl of CF sputum or PBS control was added and
205 allowed to settle. 200 μl of SLPI functionalised nanoparticles (10 mg/ml) were added to the sputum
206 and PBS control wells with SLPI at a concentration of 100 μg/ml. Non-conjugated rhodamine loaded
207 nanoparticles were diluted to give an equivalent concentration of rhodamine. Particle penetration
208 was measured over 24 h after which the gelatin layers were washed (PBS x 6) and the gelatin was
209 melted and fluorescence measured at 480/520 nm. Penetration in CF mucus was measured by
210 comparison to the PBS control which was measured as 100% penetration. Fluorescent values were
211 analysed in reference to Rhodamine 6G standards in the range (0-1000 ng/ml).

212 *2.12. Statistical analysis*

213 Results were analysed with GraphPad Prism, version 5.03, GraphPad Software (San Diego,
214 USA). T-test and one-way ANOVA analyses were performed. Statistical significance critical values
215 were defined as $^{**}P < 0.01$, $^{***}P<0.0001$.

216 **3. Results and Discussion**

217 We have an interest in the development of nanoparticles designed for therapeutic application in
218 diseases such as Cystic Fibrosis (CF) [35].

3.1. Nanoparticle preparation and tobramycin loading and release

Various microparticle-/nanoparticle-based drug delivery systems have been developed to facilitate the effective delivery of drugs to the pulmonary system [36]. Here we report the development of tobramycin-loaded nanoparticles composed of alginate and chitosan. The results of varying the ratio of the components (alginate:chitosan:tobramycin:$CaCl_2$) on particle formation are reported in **Table 1**.

Table 1. Optimisation of formulation parameters in the design of alginate/chitosan nanoparticles. Results presented as mean ± S.D, N = 3.

Alginate (w/w ratio)	Chitosan (w/w ratio)	Tobramycin (w/w ratio)	$CaCl_2$ (w/w ratio)	Aggregation
9	1.5	1.5	3	Yes
9	1.5	1.5	0.8	Yes
9	0.8	0.8	0	No
9	1	3	0	Yes
9	1	1.5	0	No

During the optimization studies we observed that a higher concentration of cations in the formulation resulted in the aggregation of the nanoparticles (**Table 1**). The optimal formulation of alginate:chitosan:tobramycin 9:1:1.5 (w/w/w), resulted in the formation of nanoparticles with a fairly narrow size distribution and high loading of tobramycin (**Table 2, Figure S1** and **Figure S2**) and was therefore used for further studies. The nanoparticle size distribution assessed by DLS measurements (**Table 2, Figure S1**) were somewhat larger than those observed by TEM (**Figure S2**), however, the DLS data was judged to be more representative of the whole population of nanoparticles.

Table 2. Properties of the nanoparticles prepared with the optimal formulation of alginate:chitosan:tobramycin (9:1:1.5, w/w/w). Results presented as mean ± S.D, N = 3.

Particle size (nm)	PDI	Zeta potential (mV)	Tobramycin loading in nanoparticles (μg/mg)	% entrapment
437.5 ± 22.3	0.27 ± 0.07	21.6 ± 1.1	74.2 ± 3.4	44.5 ± 2.0

Tobramycin loading (**Table 2**) and release (**Figure S3**) was quantified by fluorimetry after derivatization of the tobramycin with ortho-phthaldialdehyde [37] (the calibration curve is depicted in **Figure S4**); a typical biphasic release was observed with 18.9% of the entrapped tobramycin released within the first 24 h, although the overall release was limited to 25.4% of the total amount of loaded tobramycin over the course of the experiment. The optimal formulation of the tobramycin-loaded alginate/chitosan nanoparticles was tested against live cultures of *P. aeruginosa* (**Figure 2**). The unloaded nanoparticles showed no activity against *P. aeruginosa*, tobramycin alone had an MIC of 1.5 μg/ml, and the tobramycin-loaded nanoparticles showed activity in a dose dependent manner as expected (with a somewhat elevated MIC of 6.25 μg/ml which is likely to be due to the rate of diffusion of tobramycin from the nanoparticles).

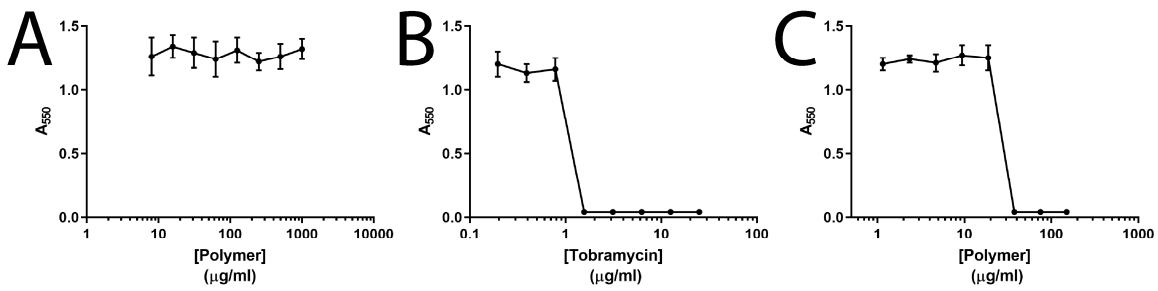

Figure 2. MIC analysis of tobramycin-loaded alginate/chitosan nanoparticles against *P. aeruginosa*. A) Unloaded nanoparticle control. B) Free tobramycin. C) Tobramycin loaded nanoparticles. Mean values ± S.D, N = 3.

3.2. SLPI-conjugated nanoparticle preparation and interactions with model biological milieu

Disease states such as CF are characterized by increased infiltration of pro-inflammatory cytokines in the lung [25] which leads to extensive tissue damage through NE mediated activity [12]. As a natural inhibitor of NE [31] it was anticipated that the conjugation of SLPI to the nanoparticles could potentially inhibit NE mediated tissue destruction while also achieving passive targeting for the particles. The properties of nanoparticles prepared with SLPI in the absence/presence of carbodiimide crosslinker are displayed in **Table 3** (and **Figure S5**), with nanoparticles formed in the absence of carbodiimide containing 0.2 μg of SLPI, whereas those formed in the presence of carbodiimide containing 11.2 μg of SLPI, highlighting the necessity of using the carbodiimide to attach the SLPI to the nanoparticles.

Table 3. Nanoparticle properties following preparation without/with carbodiimide. Results presented as mean ± S.D, N = 3.

Crosslinker (EDC)	Particle size (nm)	PDI	Zeta potential (mV)	Conjugated SLPI (μg) in nanoparticles (mg), (μg/mg)
No	437.5 ± 26.5	0.26 ± 0.09	-22.9 ± 3.1	0.2 ± 0.3
Yes	458.0 ± 31.1	0.31 ± 0.12	-19.2 ± 2.1	11.2 ± 2.3

To evaluate whether any of the conjugated SLPI was functional after conjugation to the chitosan in the nanoparticles, the SLPI-conjugated nanoparticles were incubated with human neutrophil elastase (NE) and their ability to inhibit the cleavage of a chromogenic substrate (methoxysuccinyl-Ala-Ala-Pro-Val-P-nitroanilide) was studied [38] and compared to free SLPI and unmodified nanoparticles (**Figure 3**). The unmodified/blank alginate/chitosan nanoparticles show very little NE inhibitory activity (similar to NE alone), by contrast the SLPI conjugated particles displayed a similar level of activity as the free SLPI, confirming that the SLPI retains NE inhibitory activity when conjugated to the nanoparticles.

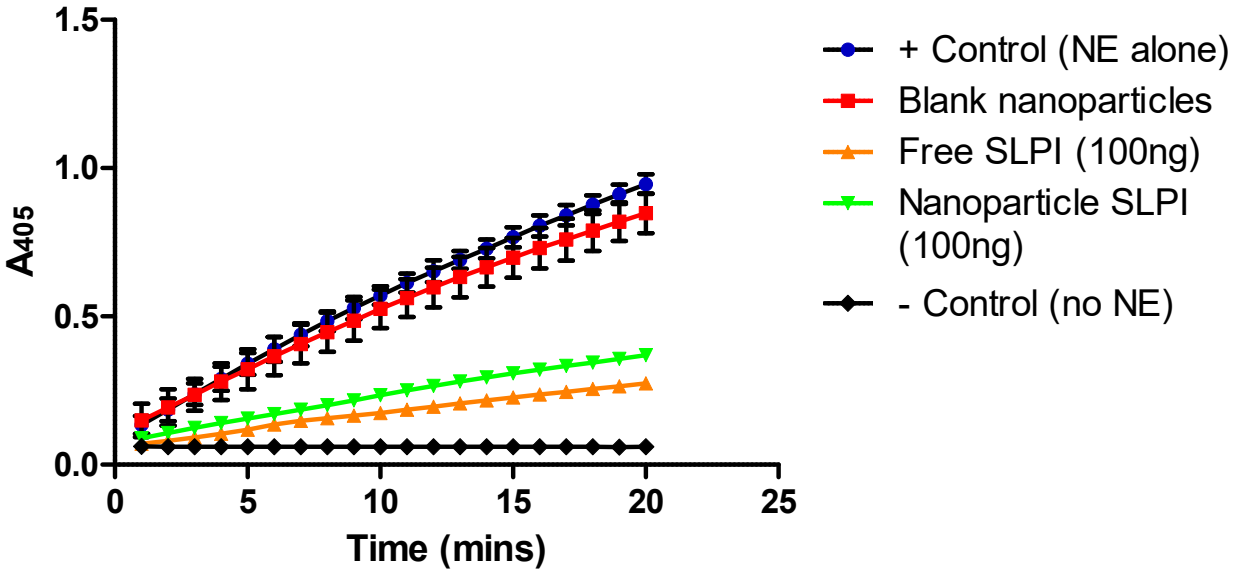

Figure 3. Inhibition of NE by SLPI-conjugated nanoparticles. Results presented as mean ± S.D, N = 3.

In order to effectively treat *P. aeruginosa* infections it is necessary for drugs to achieve therapeutic concentrations at the site of bacterial colonization. *P. aeruginosa* has been shown to reside within the thick mucus secretions within the CF lung [39]. We anticipated the conjugation of SLPI to the nanoparticles could enhance their mucoadhesive properties via electrostatic interactions [40]. The penetration of SLPI-conjugated nanoparticles into CF mucus was assessed using rhodamine-loaded nanoparticles (**Figure 4 and Figure S6**) in accordance with a literature protocol [41]. We observed that the SLPI conjugaed nanoparticles entrapping rhodamine dye were retained to a greater level in CF sputum over the non-conjugated particles. Only 19.4% of nanoparticles functionalised with SLPI were shown to traverse CF mucus as opposed to 29.7% of particle without SLPI (in line with literature showing nanoparticles with cationic coatings could be retained within the pulmonary environment longer, thereby increasing the therapeutic efficacy of the drug) [42].

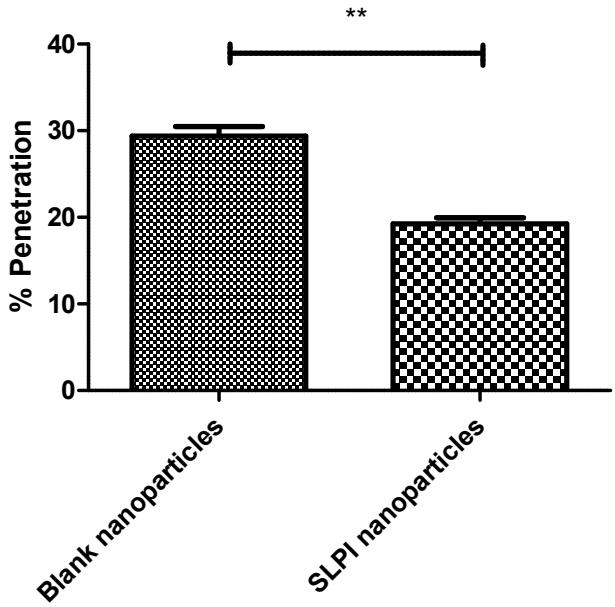

Figure 4. Ability of rhodamine loaded nanoparticles to penetrate CF mucus. Mean ± S.D, N = 3, (**P<0.01).

5. Conclusions

The complexity of CF treatment regimens has been shown to be largely responsible for patient non-compliance [19,43], and the formulation of nanoparticles displaying mucoadhesive properties is a potential solution to minimizing problems associated with non-compliance, with potentially significant beneficial economic, health and societal impacts at the global scale. The nanoparticles described herein were capable of delivering a potent antimicrobial (tobramycin) to *P. aeruginosa*, and the conjugation of SLPI enhanced their mucoadhesive properties [39, 42] potentially increasing the efficacy of drug delivery over prolonged periods, and potentially thereby helping minimize problems associated with non-compliance after successful pre-clinical and clinical studies [44,45].

Supplementary Materials: The following are available online at www.mdpi.com/xxx/s1, Figure S1. DLS analysis of the nanoparticles prepared with the optimal formulation of alginate:chitosan:tobramycin (9:1:1.5, w/w/w). Figure S2. TEM analysis of alginate/chitosan nanoparticles. Figure S3. Cumulative release of tobramycin release from alginate/chitosan nanoparticles. Figure S4. Calibration curve for tobramycin sulphate in nanoparticle supernatant following formulation of tobramycin loaded alginate/chitosan nanoparticles. Figure S5. Calibration curve for SLPI in the range (31.25 – 500 μg/ml) quantified with the BCA assay kit (Pierce, UK). Figure S6. Standard curve of Rhodamine 6G in the concentration range (0-1000 ng/ml).

Author Contributions: Conceptualization, C.C.T., C.J.S., J.S.E., and M.E.M.; methodology, all authors; formal analysis, all authors; investigation, all authors; data curation, M.H., M.E.M.; writing—original draft preparation, M.H. and J.G.H.; writing—review and editing, all authors; supervision, M.E.M.; project administration, M.E.M.; funding acquisition, M.E.M.

Funding: This research was supported by: a PhD studentship from Queen's University Belfast for M.H.; Lancaster University for a Faculty of Science and Technology Early Career Internal Grant to support collaborative interactions between J.G.H. and M.E.M.; a MRC Proximity to Discovery grant (MC_PC_17192) for supporting interactions with J.G.H. and E.A.S.; the UK Engineering and Physical Sciences Research Council (EPSRC, EP/H031065/1) to support C.C.T, C.J.S, J.S.E and M.E.M and an Innovate UK Knowledge Transfer Partnership to support M.T. The APC was funded by M.E.M. at the University of South Alabama.

Acknowledgments: We thank Professor Colin McCoy for access to a BMG-Labtech Fluorstar Optima fluorescent plate reader.

Conflicts of Interest: The authors declare no conflict of interest. The funders had no role in the design of the study; in the collection, analyses, or interpretation of data; in the writing of the manuscript, and in the decision to publish the results.

References

1. Dulhanty, A. M.; Chang, X. B.; Riordan, J. R. Mutation of potential phosphorylation sites in the recombinant R domain of the cystic fibrosis transmembrane conductance regulator has significant effects on domain conformation. *Biochem. Biophys. Res. Commun*. **1995**, 206, 207–214. DOI: 10.1006/bbrc.1995.1029.
2. Riordan, J. R.; Rommens, J. M.; Kerem, B.; Alon, N.; Rozmahel, R.; Grzelczak, Z.; Chou, J. L. Identification of the cystic fibrosis gene: cloning and characterization of complementary DNA. *Science* **1989**, 245, 1066–73. DOI: 10.1126/science.2475911.
3. Marino, C. R.; Matovcik, L. M.; Gorelick, F. S.; Cohn, J. A. Localization of the cystic fibrosis transmembrane conductance regulator in pancreas. *J. Clin. Invest*. **1991**, 88, 712–6. DOI: 10.1172/JCI115358.
4. Jacquot, J.; Puchelle, E.; Hinnrasky, J.; Fuchey, C.; Bettinger, C.; Spilmont, C.; Pavirani, A. Localization of the cystic fibrosis transmembrane conductance regulator in airway secretory glands. *Eur. Resp. J*. 1993, 6, 169–76.
5. Sbarbati, A.; Bertini, M.; Catassi, C.; Gagliardini, R.; Osculati, F. Ultrastructural lesions in the small bowel of patients with cystic fibrosis. *Ped. Res*. **1998**, 43, 234–9. DOI: 10.1203/00006450-199804001-01393.
6. Kreda, S. M.; Mall, M.; Mengos, A.; Rochelle, L.; Yankaskas, J.; Riordan, J. R.; Boucher, R. C. Characterization of wild-type and deltaF508 cystic fibrosis transmembrane regulator in human respiratory epithelia. *Mol. Biol. Cell*, **2005**, 16, 2154–67. DOI: 10.1091/mbc.e04-11-1010.
7. Krouse, M. E. Is cystic fibrosis lung disease caused by abnormal ion composition or abnormal volume? The *J. Gen. Physiol.* **2001**, 118, 219–22.

8. Stenbit, A. E.; Flume, P. A. Pulmonary exacerbations in cystic fibrosis. *Curr. Opin. Pulm. Med*. **2011**, 17, 442–7. DOI: 10.1097/MCP.0b013e32834b8c04.
9. Mall M.; Boucher R. Pathogenesis of Pulmonary Disease in Cystic Fibrosis. In Cystic Fibrosis in the 21st Century. Bush A.; Alton, E. W. F. W.; Davies, J.C.; Griesenbach, U.; Jaffe, A., Eds; Prog Respir Res. Karger: Basel, Switzerland, **2006**; Volume 34, pp. 116-121, ISBN: 978-3-8055-7960-5. DOI:10.1159/000088489.
10. Haley, C. L.; Colmer-Hamood, J. A.; Hamood, A. N. Characterization of biofilm-like structures formed by Pseudomonas aeruginosa in a synthetic mucus medium. *BMC Microbiol*., **2012**, 12, 181. DOI: 10.1186/1471-2180-12-181.
11. May, T. B.; Shinabarger, D.; Maharaj, R.; Kato, J.; Chu, L.; DeVault, J. D.; Rothmel, R. K. Alginate synthesis by Pseudomonas aeruginosa: a key pathogenic factor in chronic pulmonary infections of cystic fibrosis patients. *Clin. Microbiol. Rev.* **1991**, 4, 191–206. DOI: 10.1128/cmr.4.2.191.
12. Quinn, D. J.; Weldon, S.; Taggart, C. C. Antiproteases as therapeutics to target inflammation in cystic fibrosis. *Open Respir. Med. J.*, **2010**, 4, 20–31. DOI: 10.2174/1874306401004010020.
13. Høiby, N.; Ciofu, O.; Bjarnsholt, T. Pseudomonas aeruginosa biofilms in cystic fibrosis. *Future Microbiol.* **2010**, 5, 1663–74. DOI: 10.2217/fmb.10.125.
14. Cystic fibrosis: diagnosis and management. Available online: https://www.nice.org.uk/guidance/ng78/chapter/Recommendations#pulmonary-monitoring-assessment-and-management (accessed on 30 06 2019).
15. Tobramycin. Available online: https://bnf.nice.org.uk/drug/tobramycin.html (accessed on 30 06 2019).
16. Omri, A.; Beaulac, C.; Bouhajib, M.; Montplaisir, S.; Sharkawi, M.; Lagacé, J. Pulmonary retention of free and liposome-encapsulated tobramycin after intratracheal administration in uninfected rats and rats infected with Pseudomonas aeruginosa. *Antimicrob. Agents Chemother.* **1994**, 38, 1090–5. DOI: 10.1128/AAC.38.5.1090.
17. Smyth, A.; Walters, S. Prophylactic antibiotics for cystic fibrosis. *Cochrane Database Syst. Rev*. **2003**, 3, CD001912. DOI: 10.1002/14651858.CD001912.
18. Girón Moreno, R. M.; Salcedo Posadas, A.; Mar Gómez-Punter, R. Inhaled antibiotic therapy in cystic fibrosis. *Archivos de Bronconeumología*, **2011**, 47, 14–8. DOI: 10.1016/S0300-2896(11)70031-X.
19. IM2 Cystic Fibrosis Patient Adherence (Adult). https://www.england.nhs.uk/wp-content/uploads/2016/11/im2-cystic-fibrosis-patient-adherence.pdf (accessed on 30 06 2019).
20. Selimoglu, E. Aminoglycoside-induced ototoxicity. *Curr. Pharm. Des*. **2007**, 13, 119–26. DOI: 10.2174/138161207779313731.
21. Kumin, G. D. Clinical Nephrotoxicity of Tobramycin and Gentamicin. *JAMA*, **1980**, 244, 1808. DOI: 10.1001/jama.1980.03310160024018.
22. Tobramycin 300 mg/ 5 ml nebuliser solution. Available online: https://www.medicines.org.uk/emc/product/2683/smpc (accessed on 30 06 2019).
23. Ramphal, R.; Lhermitte, M.; Filliat, M.; Roussel, P. The binding of anti-pseudomonal antibiotics to macromolecules from cystic fibrosis sputum. *J. Antimicrob. Chemother*. **1988**, 22(4), 483–90. DOI: 10.1093/jac/22.4.483.
24. Mall, M.; Grubb, B. R.; Harkema, J. R.; O'Neal, W. K.; Boucher, R. C. Increased airway epithelial Na+ absorption produces cystic fibrosis-like lung disease in mice. *Nature Medicine*, **2004**, 10, 487–93. DOI: 10.1038/nm1028.
25. Heeckeren, A.; Walenga, R.; Konstan, M. W.; Bonfield, T.; Davis, P. B.; Ferkol, T. Excessive inflammatory response of cystic fibrosis mice to bronchopulmonary infection with Pseudomonas aeruginosa. *J. Clin. Invest.* **1997**, 100, 2810–5. DOI: 10.1172/JCI119828.
26. King, A. E.; Critchley, H. O.; Kelly, R. W. Presence of secretory leukocyte protease inhibitor in human endometrium and first trimester decidua suggests an antibacterial protective role. *Mol. Hum. Reprod*. **2000**, 6, 191–6. DOI: 10.1093/molehr/6.2.191.
27. Appelhans, B.; Ender, B.; Sachse, G.; Nikiforov, T.; Appelhans, H.; Ebert, W. Secretion of antileucoprotease from a human lung tumor cell line. *FEBS Lett*. **1987**. 224, 14–18. DOI: 10.1016/0014-5793(87)80413-1.
28. Franken, C.; Meijer, C. J.; Dijkman, J. H. Tissue distribution of antileukoprotease and lysozyme in humans. *J. Histochem. Cytochem*. **1989**, 37, 493–8. OI:10.1177/37.4.2926127.

394 29. Heinzel, R.; Appelhans, H.; Gassen, G.; Seemüller, U.; Machleidt, W.; Fritz, H.; Steffens, G. Molecular
395 cloning and expression of cDNA for human antileukoprotease from cervix uterus. *Eur. J. Biochem*. **1986**,
396 160, 61–7. DOI: 10.1111/j.1432-1033.1986.tb09940.x.
397 30. Lee, C. H.; Igarashi, Y.; Hohman, R. J.; Kaulbach, H.; White, M. V.; Kaliner, M. A. Distribution of secretory
398 leukoprotease inhibitor in the human nasal airway. *Am. Rev. Respir. Dis*. **1993**, 147, 710–6. DOI:
399 10.1164/ajrccm/147.3.710.
400 31. Thompson, R. C.; Ohlsson, K. Isolation, properties, and complete amino acid sequence of human secretory
401 leukocyte protease inhibitor, a potent inhibitor of leukocyte elastase. *Proc. Natl. Acad. Sci. USA* **1986**, 83,
402 6692–6. DOI: 10.1073/pnas.83.18.6692.
403 32. McElvaney, N. G.; Nakamura, H.; Birrer, P.; Hébert, C. A.; Wong, W. L.; Alphonso, M.; Crystal, R. G.
404 Modulation of airway inflammation in cystic fibrosis. In vivo suppression of interleukin-8 levels on the
405 respiratory epithelial surface by aerosolization of recombinant secretory leukoprotease inhibitor. *J. Clin.*
406 *Invest*. **1992**, 90, 1296–301. DOI: 10.1172/JCI115994.
407 33. McElvaney, N. G.; Doujaiji, B.; Moan, M. J.; Burnham, M. R.; Wu, M. C.; Crystal, R. G. Pharmacokinetics of
408 recombinant secretory leukoprotease inhibitor aerosolized to normals and individuals with cystic fibrosis.
409 *Am. Rev. Respir. Disease*, **1993**, 148, 1056–60. DOI: 10.1164/ajrccm/148.4_Pt_1.1056.
410 34. Taggart, C. C.; Cryan, S.-A.; Weldon, S.; Gibbons, A.; Greene, C. M.; Kelly, E.; McElvaney, N. G. Secretory
411 leucoprotease inhibitor binds to NF-kappaB binding sites in monocytes and inhibits p65 binding. *J. Exp.*
412 *Med*. **2005**, 202, 1659–68. DOI: 10.1084/jem.20050768.
413 35. Hill, M.; Cunningham, R. N.; Hathout, R. M.; Johnston, C.; Hardy, J. G.; Migaud, M. E. Formulation of
414 antimicrobial tobramycin loaded PLGA nanoparticles via complexation with AOT. *Journal of Functional*
415 *Biomaterials*. **2019**, 10, 26.
416 36. Mansour, H. M.; Rhee, Y.-S.; Wu, X. Nanomedicine in pulmonary delivery. *Int. J. Nanomed*. **2009**, 4, 299–
417 319. DOI: https://doi.org/10.2147/IJN.S4937.
418 37. Benson, J. R.; Hare, P. E. O-phthalaldehyde: fluorogenic detection of primary amines in the picomole
419 range. Comparison with fluorescamine and ninhydrin. Proc. Natl. Acad. Sci. USA 1975, 72, 619–22. DOI:
420 10.1073/pnas.72.2.619.
421 38. Weldon, S.; McNally, P.; McElvaney, N. G.; Elborn, J. S.; McAuley, D. F.; Wartelle, J.; Taggart, C. C.
422 Decreased levels of secretory leucoprotease inhibitor in the Pseudomonas-infected cystic fibrosis lung are
423 due to neutrophil elastase degradation. *J. Immunol*. **2009**, 183, 8148–56. DOI: 10.4049/jimmunol.0901716.
424 39. Baltimore, R. S.; Christie, C. D.; Smith, G. J. Immunohistopathologic localization of Pseudomonas
425 aeruginosa in lungs from patients with cystic fibrosis. Implications for the pathogenesis of progressive
426 lung deterioration. *Am. Rev. Respir. Dis*. **1989**, 140, 1650–61. DOI: 10.1164/ajrccm/140.6.1650.
427 40. Hirano, M.; Kamada, M.; Maegawa, M.; Gima, H.; Aono, T. Binding of human secretory leukocyte
428 protease inhibitor in uterine cervical mucus to immunoglobulins: pathophysiology in immunologic
429 infertility and local immune defense. *Fertil. Steril.* **1999**, 71, 1108–14. DOI: 10.1016/S0015-0282(99)00142-9.
430 41. Ungaro, F.; d'Angelo, I.; Coletta, C.; d'Emmanuele di Villa Bianca, R.; Sorrentino, R.; Perfetto, B.; Quaglia,
431 F. Dry powders based on PLGA nanoparticles for pulmonary delivery of antibiotics: modulation of
432 encapsulation efficiency, release rate and lung deposition pattern by hydrophilic polymers. *J. Control.*
433 *Release*, **2012**, 157, 149–59. DOI: 0.1016/j.jconrel.2011.08.010.
434 42. Yamamoto, H.; Kuno, Y.; Sugimoto, S.; Takeuchi, H.; Kawashima, Y. Surface-modified PLGA nanosphere
435 with chitosan improved pulmonary delivery of calcitonin by mucoadhesion and opening of the
436 intercellular tight junctions. *J. Control. Release* **2005**, 102, 373–81. DOI: 10.1016/j.jconrel.2004.10.010.
437 43. Dodd, M. E., & Webb, A. K. Understanding non-compliance with treatment in adults with cystic fibrosis. *J.*
438 *R. Soc. Med*. **2000**, 93, 2–8.
439 44. Fisher, J. T.; Zhang, Y.; Engelhardt, J. F. Comparative biology of cystic fibrosis animal models. *Methods Mol.*
440 *Biol*. **2011**, 742, 311–34. DOI: 10.1007/978-1-61779-120-8_19.
441 45. Pezzulo, A. A.; Tang, X. X.; Hoegger, M. J.; Alaiwa, M. H. A.; Ramachandran, S.; Moninger, T. O.; Zabner,
442 J. Reduced airway surface pH impairs bacterial killing in the porcine cystic fibrosis lung. *Nature* **2012**, 487,
443 109–13. DOI: 10.1038/nature11130.